Title

Assessing the Outcomes of Focused Heating of the Skin by a Long-Pulsed 1064 nm Laser with an Integrated Scanner, Infrared Thermal Guidance, and Optical Coherence Tomography

Journal

Lasers in Surgery and Medicine, 53(6)

ISSN

0196-8092

Authors

Mehrabi, Joseph N
Kelly, Kristen M
Holmes, Jon D
et al.

Publication Date

2021-08-01

DOI

10.1002/lsm.23377

Assessing the Outcomes of Focused Heating of the Skin by a Long-Pulsed 1064 nm Laser with an Integrated Scanner, Infrared Thermal Guidance, and Optical Coherence Tomography

Joseph N. Mehrabi, MS,[1] Kristen M. Kelly, MD,[1,2] Jon D. Holmes, MS,[3] and Christopher B. Zachary, MBBS, FRCP[1]*

[1]*Department of Dermatology, University of California Irvine, Irvine, California 92697*
[2]*Beckman Laser Institute, Laser Microbeam and Medical Program, University of California Irvine, Irvine, California 92612*
[3]*Michelson Diagnostics Ltd., Maidstone, ME14 3EN, UK*

Background and Objective: Long-term benefits can be predicted by the incorporation of more intelligent systems in lasers and other devices. Such systems can produce more reliable zones of thermal injury when used in association with non-invasive monitoring and precise laser energy delivery. The more classical endpoint of tumor destruction with radiofrequency or long-pulsed (LP) 1064 nm laser is the non-specific appearance of tissue graying and tissue contraction. Herein we discuss combining non-invasive LP 1064 nm Nd:YAG treatment with the assistance of optical coherence tomography (OCT) and the forward-looking infrared (FLIR) thermal camera while testing literature-based formulae for thermal destruction.

Study Design/Materials and Methods: The skin on the forearm and back of two consenting volunteers was marked and anesthetized with lidocaine with epinephrine. The parameters of a scanner-equipped LP 1064 nm Nd:YAG laser were adjusted to achieve an epidermal/superficial dermal heating of between 50°C and 60°C over a specified time course. Experimental single treatments examined various adjusted parameters including, fluence, pulse overlap, pulse duration, scan size, and pulse rate. A FLIR camera was used to record skin temperature. Outcome measures included skin temperature, post-treatment appearance, and OCT assessment of skin and vascular damage. The clinical response of each treatment was followed daily for 4 weeks.

Results: Optimal protocols initially raised the skin temperature to between 55°C and 60°C, which was carefully maintained using subsequent laser passes over a 60-second time course. Immediately post laser, clinical responses included erythema, edema, and blistering. Immediate OCT revealed increased vascularity with intact, dilated blood vessels. Prolonged exposure above 60°C resulted in subepidermal blistering and an absence of blood flow in the treatment area with prolonged healing.

Conclusion: The LP 1064 nm laser can be used to achieve heat-related tissue injury, though the narrow parameters necessary for the desired endpoint require the assistance of IR thermal regulation to avoid unacceptable outcomes. The use of the laser scanner ensures precise energy delivery over a defined treatment area. Future studies might explore this as a selective hyperthermic method for the treatment of non-melanoma skin cancer. Lasers Surg. Med.

Key words: heating; long-pulse 1064nm laser; Nd:YAG; optical coherence tomography; thermal monitoring

INTRODUCTION

There are multiple methods to induce thermal injury in the skin, including lasers, ultrasound, and radiofrequency. Many of these are uncontrolled, potentially resulting in undesirable burns and subsequent scarring. Controlled cutaneous heating is commonly employed in dermatology for an array of applications, such as skin resurfacing and rejuvenation, hair removal, tattoo and pigment elimination, and vessel coagulation.

Most laser interactions with the skin involve heat, raising the temperature and denaturing proteins, DNA, RNA, and cell membranes, and impairing cellular function. Undisciplined thermal coagulation will almost certainly lead to necrosis and a burn. Most cells can withstand temperatures up to 40°C, however, exposure time and peak temperature dictate cellular survival. Sub-lethal heat exposure can induce a heat-shock response resulting in the production of heat-shock proteins potentiating the cells'

Conflict of Interest Disclosures: All authors have completed and submitted the ICMJE Form for Disclosure of Potential Conflicts of Interest and none were reported.
*Correspondence to: Christopher B. Zachary, MBBS, FRCP, Department of Dermatology, University of California, Irvine, 118 Med Surge I, Irvine, CA 92617. E-mail: czachary@hs.uci.edu
Accepted 30 December 2020
Published online 00 Month 2020 in Wiley Online Library (wileyonlinelibrary.com).
DOI 10.1002/lsm.23377

resistance to thermal injury [1]. The Arrhenius model describes how the rate of cellular damage is exponentially proportional to the rise in temperature [2–6], so that even a modest increase in temperature for a given time can produce a dramatic increase in thermal injury, and also a similarly modest reduction in temperature can result in no injury. Therefore, control of temperature is critical to achieving the desired level of thermal damage in the targeted tissue.

Laser treatment of skin cancer has been studied in multiple publications [7,8]. The long-pulse Nd:YAG has been used to achieve clearing of skin cancers, but prior work reports variable and unpredictable degrees of scarring and on occasions significant collateral damage [9,10]. This is not surprising, given the sensitivity to temperature of tissue damage predicted by the Arrhenius model. To our knowledge, previous studies have not attempted to objectively determine parameters for maximum tumor destruction with minimal surrounding skin injury. In this study, we used optical coherence tomography (OCT) and infrared thermal imaging to measure the immediate and long-term effects of LP Nd:YAG with varied treatment parameters, and then explored the potential to control the temperature using thermal imaging camera guidance.

We hypothesize that there exists an optimal combination of temperature and time that will maximize the chance of inducing a necrotic or apoptotic response in skin tumors without causing ulceration and scarring in surrounding healthy tissue. Therefore, in this study, we set out to explore how normal healthy skin temperature responded to LP Nd:YAG laser settings, how this depended on factors such as presence or absence of local anesthesia and on anatomic location, and the potential to control the temperature and delivery time using thermal imaging guidance to achieve a desired hyperthermic treatment with minimal risk of ulceration or scarring.

MATERIALS AND METHODS

Two members of the investigation team, aged 50 and 70 years, volunteered to be subjects in the study. Both were Caucasian, one had diabetes, hypertension, and inflammatory osteoarthritis, the other had no known medical issues. Treatments were delivered using LP Nd:YAG laser (ClearScan™ 1064 nm; Sciton Inc., Palo Alto, CA) equipped with a scanner. The scanner provided options of adjusting scan pattern (1×1, 2×2, or 3×3) and overlap (0%–15%), illustrated in Figure 1, along with the scanning rate (Hz) and scan sequence pattern (sequential, random, outside-in, inside-out).

Various parts of the body including the shaved, ventral forearm, upper arm, upper back, leg, chest, and cheek were subject to the laser and post-treatment analysis; most experiments were conducted on the ventral forearm. Multiple laser sessions were scheduled to test the various parameters of the scanner-equipped LP Nd:YAG laser. The spot size was fixed at 5 mm, and the number of repeat passes could be manually performed at the discretion of the device operator or set by the repeat function as the

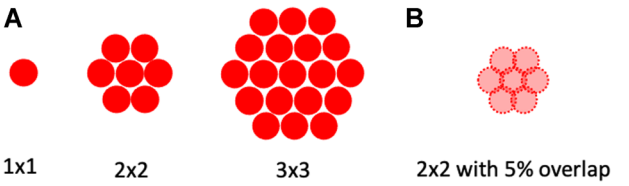

Fig. 1. (**A**) A schematic of the various scanning patterns. 1×1 emits a single 5 mm pulse, 2×2 emits 7 pulses, and 3×3 emits 19 pulses. (**B**) Scanning pattern of 2×2 with a 5% overlap. A single spot is 5 mm.

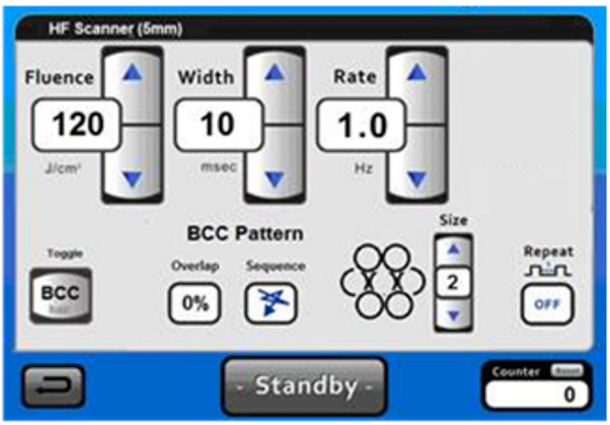

Fig. 2. A screenshot of the settings for the ClearScan™ handpiece on the Sciton LP Nd:YAG laser.

number of seconds between each scanning sequence or pass. Figure 2 depicts the screen settings of the laser with the available control parameters.

An infrared (IR) thermal camera FLIR E40 (FLIR, Wilsonville, OR) was used to record video of the treatment zone temperature and provide a continuous readout of the maximum temperature during the experiment. Each treatment area was additionally studied via OCT (VivoSight Dx; Michelson Diagnostics Ltd., Maidstone, UK) to examine the damage to the skin structure and to the underlying skin injury and vasculature pre-and post-treatment. Clinical response was followed daily and photographed weekly until each treated area fully healed.

A series of experiments were performed to evaluate the skin temperature response to different laser treatment parameters, including fluence, scan pattern size and % overlap, pulse duration, anatomical location, and use of anesthesia. These are summarized in Table 1 including the details of the settings used in each experiment.

The observed skin temperature was found to cool following an exponential curve of the form:

$$T - T_{\text{base}} = (T_{\max} - T_{\text{base}})e^{-t/k}$$

where T_{base} is the normal temperature of the skin, $T_{\max}$ is the temperature immediately after delivery of the laser pulses, t is time and k is a time constant dependent on the conditions of the experiment. Therefore it was possible to

TABLE 1. Summary of Experiments and Settings Used

Experiment	Purpose	Varied parameter	Other settings (unless otherwise stated, all with 8 ms pulse duration, 0% overlap, with anesthesia)
1	Effect of fluence	Fluence: 20, 40, 60, 80, 100, 120 J/cm^2	Pattern: 2 × 2 Location: Forearm
2	Effect of scan pattern	Scan pattern: 1 × 1 (single spot) 2 × 2 pattern 3 × 3 pattern	100 J/cm^2 15% overlap Forearm
3	Effect of anatomical locations	Back, chest, bicep, volar forearm, leg, cheek	6 × 30 J/cm^2 stacked pulses
4	Effect of pulse duration	Pulse duration: 8 ms/10 ms/15 ms/ 20 ms/30 ms/40 ms	Forearm, 2 × 2 pattern, 100 J
5	Effect of epinephrine	With and without epinephrine	120 and 130 J/cm^2 15% overlap, 2 × 2 Pattern Forearm
6	Effect of pattern overlap	Scan pattern overlap: 0%/5%	120/cm^2 2 × 2 Pattern Forearm
7	Test ability to control temperature	20, 25 J/cm^2, 30/cm^2; 2 × 2 and 3 × 3 patterns Forearm and back	

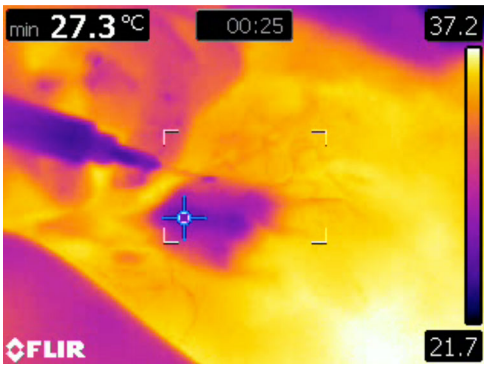

Fig. 3. An infrared image of the temperature of the skin immediately after anesthetic administration showing cooler skin area.

extract from the cooling profiles the time constant k for each experiment, and then also to calculate the time taken for the skin to cool from 60°C to 55°C.

Based on these preliminary results and then by trial and error, a novel protocol was developed, dubbed "low and slow," in which the skin was first brought up to the target temperature of 55°C with a rapid series of stacked 20–30 J/cm^2 pulses, and then further stacked 20–30 J/cm^2 "booster" pulses were delivered at intervals of 10–15 seconds to maintain the skin within the desired temperature range of 55°C–60°C for an extended period. In one experiment, the stacked pulses were delivered at predetermined intervals; in a second experiment, the stacked "booster" pulses were delivered when the FLIR camera showed that the skin temperature had fallen to the bottom of the desired temperature range (i.e., using the thermal camera readout to control the treatment). These experiments were conducted on arm and back, using 0% overlap, 8 milliseconds pulse duration, with size 2 × 2 and size 3 × 3 scan patterns.

RESULTS

Effect of Anesthesia

Subjects reported significant discomfort with the parameters used and hence anesthetic was required in order to treat with targeted higher temperatures in the 50°C–60°C range. However, lidocaine produced vasodilation (demonstrably detected by OCT) of surface vessels and so lidocaine with 1% epinephrine to combat the resulting vasodilation was administered. The use of epinephrine had no effect on the rate of cooling. Anesthetic administration cooled the target skin surface from ~34°C to ~27°C, as shown in Figure 3. Consequently, before administering treatments in later experiments the targeted area was allowed to warm for 10–15 minutes to a temperature uniform with the surrounding skin.

Effect of fluence. The maximum temperature achieved varied linearly with fluence, as would be expected. The observed temperature increase was 1.8°C per 10 J/cm^2 of fluence, demonstrated in Figure 4A.

Effect of the scan pattern. The primary impact of increasing the scan pattern size was to slow the rate of cooling of the skin. On the arm, the 3 × 3 pattern which measured 25 mm in diameter cools from 60°C to 55°C in 9.2 seconds, compared with 7.5 seconds for the 2 × 2

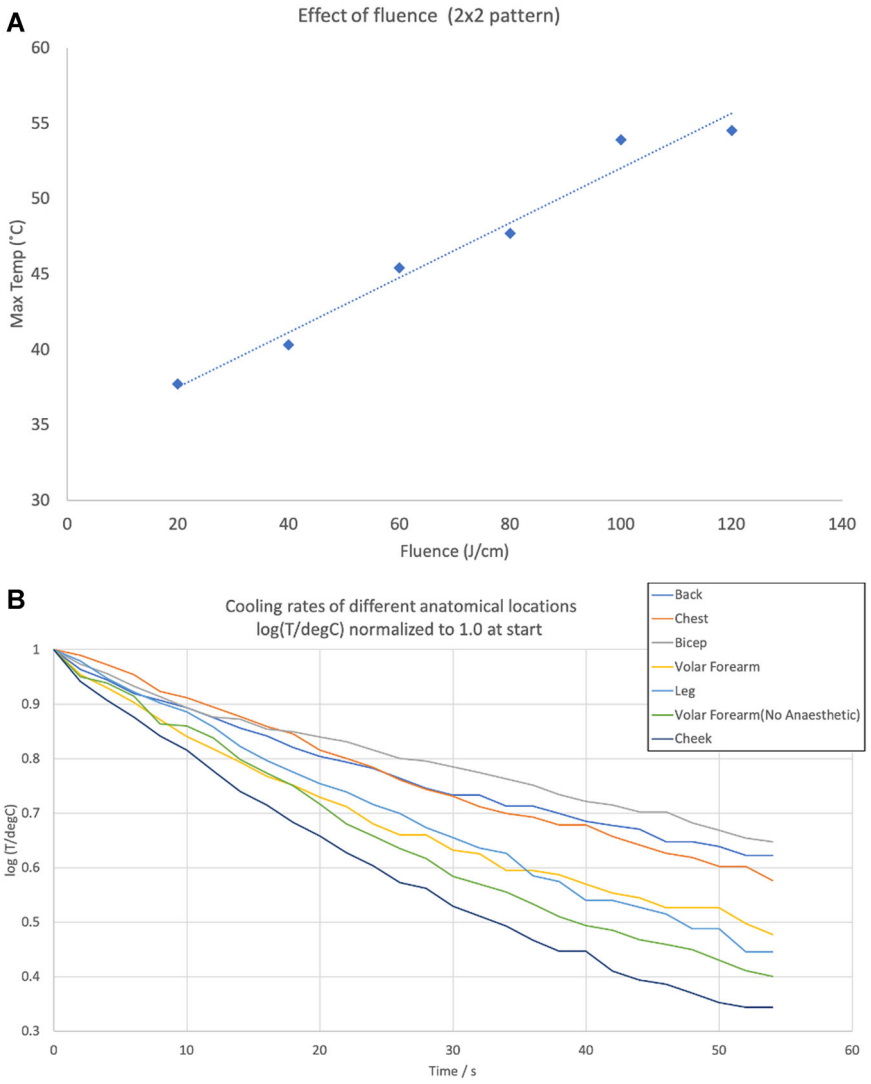

Fig. 4. Skin temperature dependence on (**A**) fluence and (**B**) cooling rate dependence on anatomical location.

pattern and just 2 seconds for a single spot, shown in Table 2.

Effect of anatomical location. The anatomical location affected both the maximum temperature reached and the rate of cooling, shown in Figure 4B and Table 2. An unanesthetized forearm was also treated for comparison. The cheek and unanesthetized forearm were observed to reach higher temperatures and had higher rates of cooling. The opposite was observed for the back, anesthetized forearm, bicep, chest, and leg.

Effect of pulse duration. No clear trend was identified regarding the effect of pulse duration. The tests at 10 and 15 milliseconds gave anomalously lower cooling coupled with purpura clinical response, but when repeated at a different place on the arm produced results similar to the other pulse durations, and this might indicate that the laser hit large vessels which affected the cooling profile.

Effect of Pattern Overlap

Unpredictable, highly variable rises in skin temperature were observed when the overlap was set beyond 10%. Accordingly, 0% overlap was used in all other experiments, providing much greater stability of tissue heating. Within a single pass and with 0% overlap, the thermal camera images of treated skin showed that the individual local hotspots from each pulse rapidly coalesced to form a single, larger area of uniform heat distribution, shown in Figure 5. Therefore 0% overlap is sufficient to treat the whole area.

Skin temperatures sustained above 60°C for more than eight seconds resulted in clinically observed and OCT-confirmed sub-epidermal blistering. The blistered areas healed demonstrating erythema, edema, scabbing, and

TABLE 2. Cooling Rates

Experiment	Description	Cooling time constant/s	Cooling time from 60°C to 55°C
2	1 × 1 Single spot	9	2.0
	2 × 2 Scan pattern	35	7.5
	3 × 3 scan pattern	45	9.2
3	Back	44	9.3
	Chest	49	10.5
	Bicep	48	10.2
	Volar forearm	30	6.4
	Leg	34	7.3
	Cheek	24	5.2
	Volar forearm (no anesthesia)	31	5.6
4	8 ms pulse duration	26	15.2
	10 ms pulse duration (a)	71	4.4
	10 ms pulse duration (b)	21	8.2
	15 ms pulse duration (a)	39	4.7
	15 ms pulse duration (b)	22	4.1
	20 ms pulse duration	19	6.8
	30 ms pulse duration	32	2.2
	40 ms pulse duration	11	5.4
5	Lidocaine, no epinephrine	31	6.6
	Lidocaine with 1% epinephrine	31	6.5

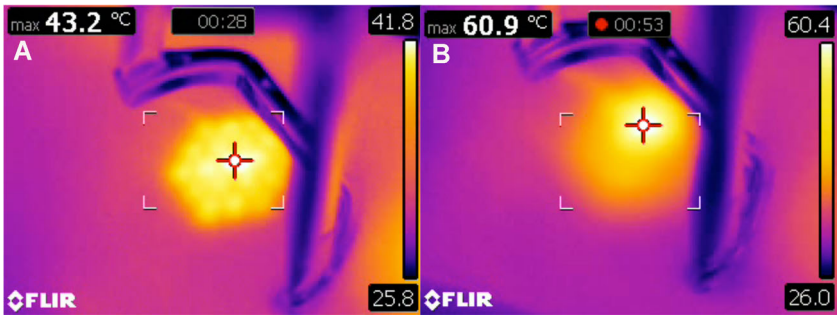

Fig. 5. Infrared images of the gradual consolidation of heat signatures from the 5th pass in a sequence (**A**) immediately after delivery of 3 × 3 pattern and (**B**) seconds later, showing thermal diffusion.

lengthy resolution of up to 8 weeks. OCT of the healing site revealed obvious scabbing and crusting with underlying reduced blood flow surrounded by increased blood flow (Fig. 6). The blisters were not reported to be tender or painful throughout the entire healing process.

Control of temperature "low and slow". Figure 7A shows observed skin temperature with "low and slow" stacked 30 J/cm^2 pulses delivered at 18 seconds fixed intervals four times after initial heating phase, on arm and back, using size 2 pattern. The temperature was maintained within 47°C–57°C range for 90 seconds on the arm, and within 50°C–59°C range for 90 seconds on the back.

Figure 7B shows observed skin temperature with stacked 25 J/cm^2 pulses delivered on arm and back with size 3 pattern, using temperature dropping below 55°C to the trigger to delivery of the next booster pulse. The temperature was maintained within 54°C–63°C for 150 seconds on the arm, and within 53°C–62°C for 150 seconds on the back. These treatments resulted in ulceration and longer healing times and were clearly too aggressive.

Clinical responses, including purpura and mild blistering, were achieved with protocols maintaining a consistent temperature between 54°C and 59°C for longer than 60 seconds; temperatures above 60°C for just over 1 second had similar responses. The most reliable protocols involved maintaining low fluence scan passes throughout the entire procedure, preferably 20–30 J/cm^2 for the initial elevation and for the maintenance passes. Maintenance passes were initiated when IR readings of skin temperature dropped below 55°C.

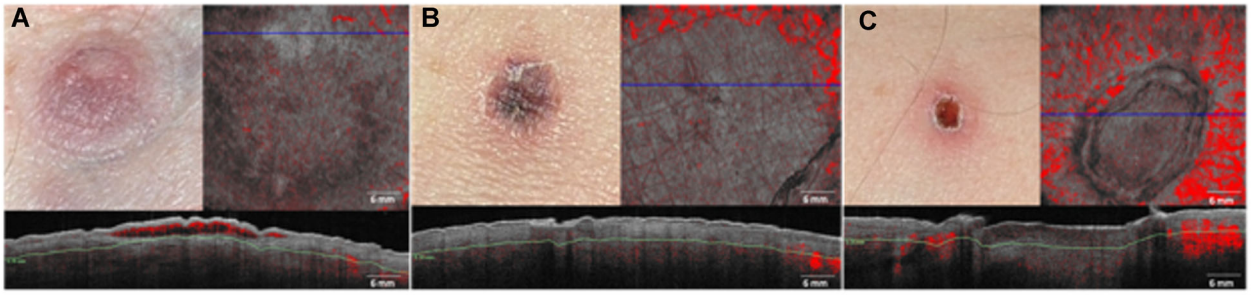

Fig. 6. Clinical pictures and en-face and cross-sectional optical coherence tomography (OCT) images of a targeted area that was heated above 60°C for longer than 5 seconds at (**A**) immediately after treatment, (**B**) 16 days after treatment, and (**C**) 5 weeks after treatment. (A) demonstrates noticeable sub-epidermal lift. Eschar formation is present in (B) with some scaling and scabbing overlying avascularity and surrounding angiogenesis. The scab had desquamated in (C) revealing mild ulceration still with avascularity and progressive surrounding angiogenesis. The depth of the en-face OCT images is acquired at 300 μm below the skin surface, capturing a skin area of 6×6 mm.

Clinical outcomes varied depending on the treated region. The back was observed to cool much more slowly than the forearm, and large blisters and scabs were observed during the recovery period. OCT of these areas immediately after treatment revealed increased vascularity with intact dilated blood vessels (Fig. 8). OCT days later demonstrated avascularity of the treated regions.

DISCUSSION

Cancer treatment with hyperthermia has been explored as a non-invasive, alternative therapeutic treatment option [11,12]. Hyperthermia has been demonstrated to induce activation of intrinsic necrotic and apoptotic pathways in a time and temperature-dependent manner. These trigger the non-conventional apoptotic pathway involving caspases 3 and 7 and the endoplasmic reticulum [13]. Pulsed dye, alexandrite, diode, and ablative lasers have exhibited efficacy in prior studies [14–26]. The LP Nd:YAG laser emits energy at a wavelength of 1064 nm in the infrared portion of the electromagnetic spectrum allowing it to penetrate to the deeper dermis and below. It is commonly used for the destruction of vascular skin lesions and hair removal with hemoglobin and melanin its target chromophores. Its ability to eradicate skin tumors has also been explored [26–30]. However, we do not believe that this process is predominantly vascular specific. Rather we believe that time and temperature-controlled thermal response achieves tumor destruction and can be controlled to protect the normal dermis and epidermis. Indeed, higher fluences and longer pulse durations are required for vascular destruction due to the relatively poor energy absorption by hemoglobin, adversely affecting the safety profile of the laser. Volumetric heating and collateral damage of uncontrolled LP 1064 nm laser treatment are common adverse reactions that would be undesired in a typical treatment with this laser. We harnessed the characteristics of this device, studying a host of laser parameters to analyze its impact on the skin. The essence of this study examined the optimal methods for providing time and temperature heating of the skin to induce necrosis of the targeted area while maintaining modest skin temperatures with the attempt to minimize blistering, scabbing, and scarring.

A series of prior studies determined that heat-related damage to the skin is temporally and temperature-dependent [2–6]. Increasing temperature leads to a rapid drop in heating time due to the exponential relationship between thermal isoeffect dosimetry and temperature [5,31]. Reduced enzyme activity, protein denaturation, and coagulation, and tissue welding occur with exposure to temperatures of 50°C, 60°C, and 70°C, respectively [32]. Table 3, showing data from Moritz et al. [5], illustrates this sensitive dependence of damage to skin temperature; at 49°C they report 9 minutes of exposure is required to achieve epidermal necrosis, falling to 30 seconds at 55°C and then just 5 seconds at 60°C. Our findings were broadly consistent with these data. This implies that to avoid full necrosis of normal skin, the tissue should not be heated to above 60°C, and also that to deliver a hyperthermic treatment in a practical time of about less than 1 minute, the temperature should be targeted around 55°C–60°C. This is a tight temperature range that places considerable demands on the method. Exceeding 60°C for even a short time risks ulceration and scarring, and conversely failing to reach 55°C may have little or no effect on the tissue. Of course, at this point, we do not know the equivalent necrotic temperature or time thresholds for non-melanoma skin cancers, and this will require further studies.

Lidocaine administration has been reported as a potentiator for thermal skin damage [33]. Skin cancer cells exposed to lidocaine were incapable of enduring the same temperature-time combinations as lidocaine-unexposed cells. In this study, the exposure times to various temperatures were on the order of one minute, therefore the effect of lidocaine was particularly difficult to examine without compromising the treated tissue. Clinically noticeable responses required higher temperatures, which required anesthesia, making it challenging to compare anesthetized treatments with the unanesthetized.

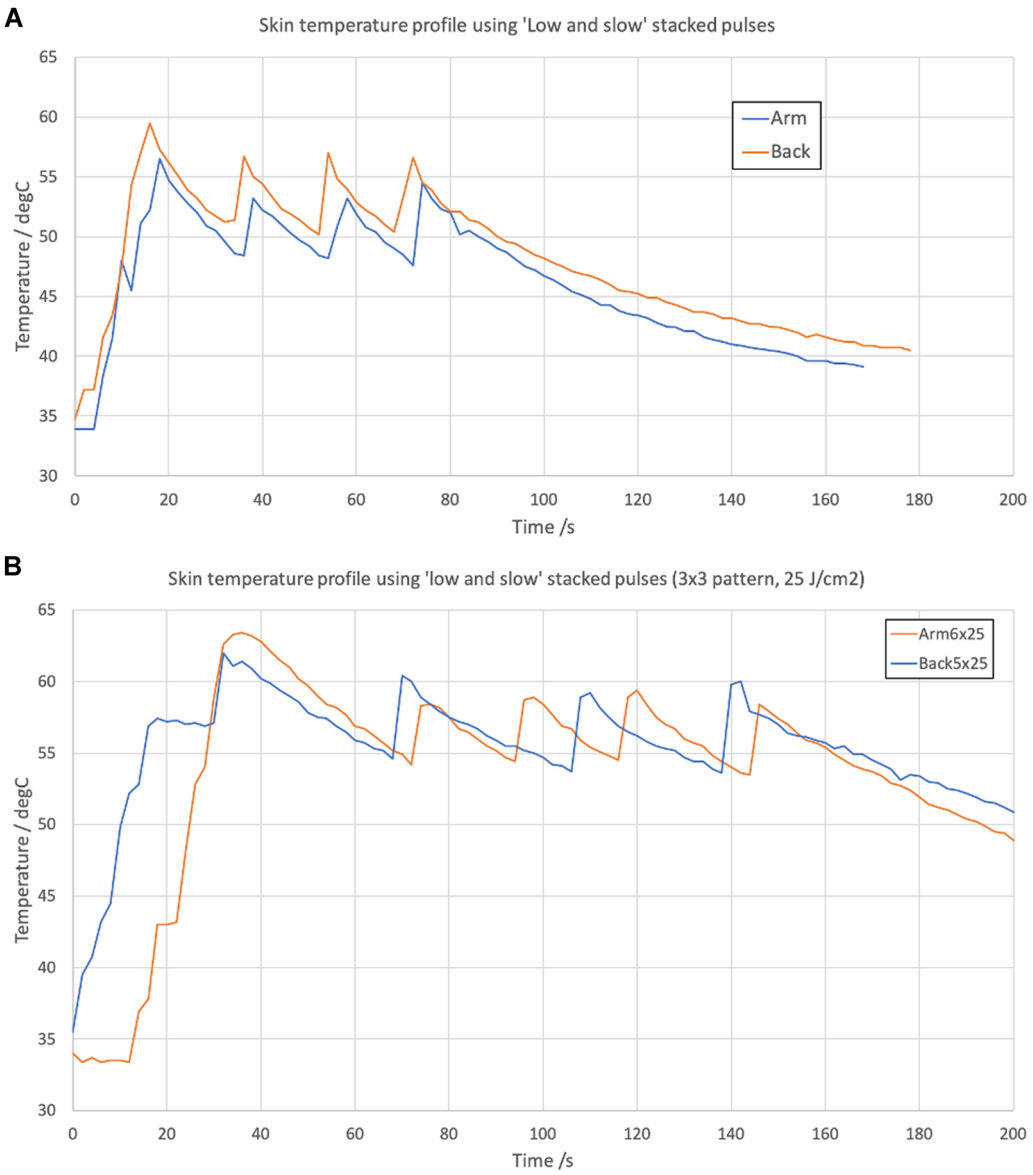

Fig. 7. Skin temperature profiles from prototype "low and slow" stacked pulse heating protocols. (**A**) 2×2 pattern, $6 \times 30\,\mathrm{J/cm^2}$ passes in rapid succession followed by three "boosters" of $30\,\mathrm{J/cm^2}$ at fixed 18 seconds time intervals. (**B**) 3×3 pattern, $8 \times 25\,\mathrm{J/cm^2}$ passes in rapid succession followed by three "boosters" of $25\,\mathrm{J/cm^2}$ using FLIR camera temperature falling to 55°C to initiate each booster.

The results from our experiments showed the key parameters to be controlled to deliver a reliable and effective thermal dose to the skin. These include laser fluence, scan pattern (i.e., size of the treated area), overlap, pulse duration, anatomical location, all of which influence both the maximum temperature reached and the cooling time, which in turn have a critical effect on tissue damage and therefore the outcome. It is therefore expected that without control of these parameters, results will be unpredictable. To combat this we devised a "low and slow" protocol designed to control the temperature within a target range 50°C–60°C, just below the threshold for full necrosis (about 60°C) over an extended period, using the long-pulsed Nd:YAG laser, and have shown proof-of-principle of this capability. Further work is required to refine and optimize this technique, ideally with automated temperature control, to achieve a tighter temperature control range.

Our original understanding was that LP 1064 nm treatment of BCCs relied upon hemoglobin absorption as its primary target to eradicate the underlying vasculature of these skin cancers. However, OCT analysis of treated tissue revealed *increased* blood flow and vasodilation when compared with untreated skin (Fig. 7). If the

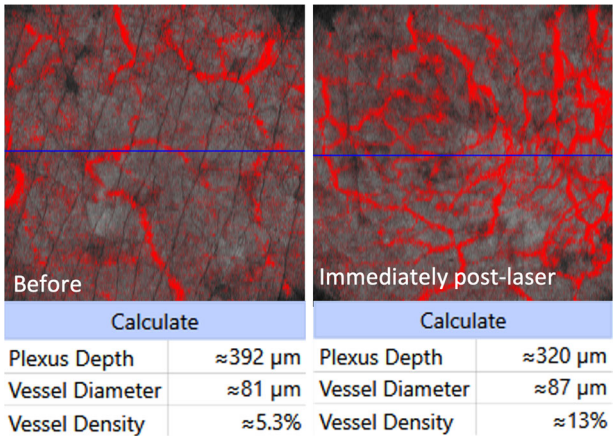

Fig. 8. The vascular profile of a 6 × 6 mm area of normal skin on the forearm (left) as compared with that of erythematous skin immediately after treatments (right) as measured with optical coherence tomography at a depth of 300 µm below the skin surface.

TABLE 3. Time Required for Full Epidermal Necrosis of Human Skin at Specified Surface Temperature, In-Vivo, Arm/Back

Temperature/°C	Time for full epidermal necrosis
45	10,800 s
49	540 s
55	30 s
60	5 s

Data from Moritz et al. [5].

improvement of BCCs is related to a vascular event, it is not an immediate process. Immediately after laser administration, an erythematous response similar to a burn was commonly observed. The response in Figure 6 occurred after more aggressive treatments where an immediate dusky blue response was noted, which resulted in mild blistering and eventual scabbing. But the vascular obliteration with surrounding angiogenesis that occurs as a result of the laser treatment is not observed until days after treatment, and completed angiogenesis and healing can take multiple weeks.

Interestingly, no pain was observed throughout the healing phase of treated areas, probably relating to a demyelinating event of sensory nerves. Although this suggests relative indiscriminate destruction, it adds to the post-operative tolerability of its administration. This combination of enhanced tolerability and indiscriminate tissue destruction has been exploited to eradicate low-risk skin cancers. Remarkable clearance and minimal recurrence have been achieved when using the LP 1064 nm laser for the treatment of basal cell carcinomas [27–30]. However, while the destruction of skin cancers with aggressive settings on a deeply penetrating laser may be clinically effective, adverse effects such as ulceration, prolonged healing, and unfavorable scarring would be inevitable and inconvenient for patients.

Therefore, this article offers an initial step for future studies attempting to explore the heat-related destruction of skin cancers using the scanner-equipped LP 1064 nm laser. This study emphasizes the use of multiple passes at low fluences in order to maintain the skin surface temperature between 51°C and 59°C for about 60 seconds. It is our suggestion that the laser engineers add IR thermal guidance as positive feedback in their software to maintain the tissue temperature much more accurately at even narrower margins such as 55-60°C. Further studies will also be required to determine how susceptible skin cancers are to "low and slow" style treatments versus the more aggressive treatments already studied [25–28].

This study is not without limitations. Only two subjects were employed, though on multiple occasions, observing the heat-related effects only on the forearm and back, whereas more vascular skin, such as that on the face, may respond differently. Reproducibility may be a challenge for other groups due to the limited production and software distribution of the Sciton ClearScan™ technology at the time of writing and the low likelihood of having an IR thermal camera available. It should be noted that laser surgeons have traditionally used handheld single pulse 1064 nm devices without the benefit and uniformity of scanning technology with precise 0% overlap. The series of experiments involved in this study were evolving as more information was learned, therefore, thorough consistency was frequently compromised in early experiments.

CONCLUSION

Hyperthermic treatment of skin cancer is in current usage, but there exist few mechanisms to control more precise heating that would simultaneously eradicate basal cell cancers and yet protect normal skin. This study set out to understand the optimal parameters to safely control hyperthermic treatment in normal skin with the LP 1064 nm laser. Important factors are laser fluence, pulse overlap, duration of the hyperthermic event, anatomic location, and anesthetic temperature. Multisequence scanned protocols offered the best control of heating when advised by IR imaging. Achieving skin surface temperatures between 51°C and 59°C for 60 seconds resulted in the optimal combination of safety and efficacy, and this was achieved with multiple laser sequences at low fluences. Future studies should implement temperature maintenance protocols to explore the heat-related destruction of skin cancers using the scanner-equipped LP 1064 nm laser with thermal guidance.

ACKNOWLEDGMENT

Equipment was provided for this study by Michelson Diagnostics Ltd. and Sciton Inc.

REFERENCES

1. Polla BS, Anderson RR. Thermal injury by laser pulses: Protection by heat shock despite failure to induce heat-shock response. Lasers Surg Med 1987;7(5):398–404.
2. Moritz AR, Henriques FC. Studies of thermal injury: II. The relative importance of time and surface temperature in the causation of cutaneous burns. Am J Pathol 1947;23(5): 695–720.
3. Moritz AR. Studies of thermal injury: III. The pathology and pathogenesis of cutaneous burns. An experimental study. Am J Pathol 1947;23(6):915–941.
4. Moritz AR, Henriques FC, Jr. Studies of thermal injury: IV. An exploration of the casualty-producing attributes of conflagrations; local and systemic effects of general cutaneous exposure to excessive circumambient (air) and circumradiant heat of varying duration and intensity. Arch Pathol 1947;43 (5):466–488.
5. Roos A, Weisiger JR, Moritz AR. Studies of thermal injury: Physiological mechanisms responsible for death during cutaneous exposure to excessive heat. J Clin Invest 1947;26(3): 505–519.
6. Henriques FC, Moritz AR. Studies of thermal injury: I. The conduction of heat to and through skin and the temperatures attained therein. A theoretical and an experimental investigation. Am J Pathol 1947;23(4):530–549.
7. Mirza FN, Khatri KA. The use of lasers in the treatment of skin cancer: A review. J Cosmet Laser Ther 2017;19(8): 451–458.
8. Soleymani T, Abrouk M, Kelly KM. An analysis of laser therapy for the treatment of nonmelanoma skin cancer. Dermatol Surg 2017;43(5):615–624.
9. Hrebinko RL. Severe injury from neodymium: Yttrium-aluminum-garnet laser therapy for penile condylomata acuminata. Urology 1996;48(1):155–156.
10. Zachary CB, Kelly KM. Lasers and other energy-based therapies. In: Bolognia JL, Schaffer JV, Cerroni L, editors. Dermatology. 4th ed. Philadelphia, PA: Elsevier; 2018 2: pp 2364–2384.
11. Hegyi G, Szigeti GP, Szasz A. Hyperthermia versus Oncothermia: Cellular effects in complementary cancer therapy. Evid Based Complement Alternat Med 2013;2013: 672873.
12. Ahmed K, Zaidi SF. Treating cancer with heat: Hyperthermia as promising strategy to enhance apoptosis. J Pak Med Assoc 2013;63(4):504.
13. Shellman YG, Howe WR, Miller LA, et al. Hyperthermia induces endoplasmic reticulum-mediated apoptosis in melanoma and non-melanoma skin cancer cells. J Invest Dermatol 2008;128(4):949–956.
14. Shah SM, Konnikov N, Duncan LM, Tannous ZS. The effect of 595 nm pulsed dye laser on superficial and nodular basal cell carcinomas. Lasers Surg Med 2009;41(6): 417–422.
15. Konnikov N, Avram M, Jarell A, Tannous Z. Pulsed dye laser as a novel non-surgical treatment for basal cell carcinomas: response and follow up 12–21 months after treatment. Lasers Surg Med 2011;43(2):72–78.
16. Minars N, Blyumin-Karasik M. Treatment of basal cell carcinomas with pulsed dye laser: A case series. J Skin Cancer 2012;2012:1–6.
17. Campolmi P, Mavilia L, Bonan P, Cannarozzo G, Lotti T. 595 nm pulsed dye laser for the treatment of superficial basal cell carcinoma. Lasers Med Sci 2005;20(3):147–148.
18. Ballard CJ, Rivas MP, McLeod MP, Choudhary S, Elgart GW, Nouri K. The pulsed dye laser for the treatment of basal cell carcinoma. Lasers Med Sci 2011;26(5):641–644.
19. Šmucler R, Vlk M. Combination of Er: YAG laser and photodynamic therapy in the treatment of nodular basal cell carcinoma. Lasers Surg Med 2008;40(2):153–158.
20. Ko DY, Kim KH, Song KH. A randomized trial comparing methyl aminolaevulinate photodynamic therapy with and without Er:YAG ablative fractional laser treatment in Asian patients with lower extremity Bowen disease: results from a 12-month follow-up. Br J Dermatol 2014;170(1):165–172.
21. Campolmi P, Brazzini B, Urso C, et al. Superpulsed CO2 laser treatment of basal cell carcinoma with intraoperatory histopathologic and cytologic examination. Dermatol Surg 2002;28(10):909–912.
22. Kavoussi H, Ebrahimi A, Rezaei M. Treatment and cosmetic outcome of superpulsed CO_2 laser for basal cell carcinoma. Acta Dermatovenerol Alp Pannonica Adriat 2013;22(3): 57–61.
23. Fitzpatrick RE, Goldman M. Treatment of superficial squamous cell carcinoma using the ultrapulse CO_2 laser: A case report. Update Dermatol Laser Surg 1993;32.
24. Fader DJ, Lowe L. Concomitant use of a high-energy pulsed CO_2 laser and a long-pulsed (810 nm) diode laser for squamous cell carcinoma in situ. Dermatol Surg 2002;28(1): 97–100.
25. Vaïsse V, Clerici T, Fusade T Bowen disease treated with scanned pulsed high energy CO2 laser. Follow-up of 6 cases. Paper presented at: Annales de dermatologie et de venereologie 2001.
26. Jalian HR, Avram MM, Stankiewicz KJ, Shofner JD, Tannous Z. Combined 585 nm pulsed-dye and 1,064 nm Nd:YAG lasers for the treatment of basal cell carcinoma. Lasers Surg Med 2014;46.1–7.
27. Ortiz AE, Anderson RR, Avram MM. 1064 nm long-pulsed Nd:YAG laser treatment of basal cell carcinoma. Lasers Surg Med 2015;47(2):106–110.
28. Ortiz AE, Anderson RR, DiGiorgio C, Jiang SIB, Shafiq F, Avram MM. An expanded study of long-pulsed 1064 nm Nd:YAG laser treatment of basal cell carcinoma. Lasers Surg Med 2018;50:727–731.
29. Ahluwalia J, Avram MM, Ortiz AE. Outcomes of long-pulsed 1064 nm Nd:YAG laser treatment of basal cell carcinoma: A retrospective review. Lasers Surg Med 2019;51(1):34–39.
30. El-Tonsy MH, El-Domyati MM, El-Sawy AE, El-Din WH, Anbar TE-DA-S, Raouf HA. Continuous-wave Nd: Yag laser hyperthermia: a successful modality in treatment of basal cell carcinoma. Dermatol Online J 2004;10(2):3.
31. Dewhirst MW, Viglianti BL, Lora-Michiels M, Hoopes PJ, Hanson M. Thermal dose requirement for tissue effect: Experimental and clinical findings. Proc SPIE Int Soc Opt Eng 2003;4954:37.
32. Dewan N. Optimisation of laser parameters for treatment of basal cell carcinoma. PhD Dissertation. 2013.
33. Raff AB, Thomas CN, Chuang GS, et al. Lidocaine-induced potentiation of thermal damage in skin and carcinoma cells. Lasers Surg Med 2019;51(1):88–94.